Histol Histopathol (2024) 39: 91-104

Histology and Histopathology
From Cell Biology to Tissue Engineering

ORIGINAL ARTICLE Open Access

REG3A overexpression functions as a negative predictive and prognostic biomarker in rectal cancer patients receiving CCRT

Wan-Shan Li[1,2,3], Tzu-Ju Chen[2,4], Sung-Wei Lee[5], Ching-Chieh Yang[6,7], Yu-Feng Tian[8], Yu-Hsuan Kuo[9,10], Hsin-Hwa Tsai[11,12,13], Li-Ching Wu[11,12], Cheng-Fa Yeh[14,15], Yow-Ling Shiue[16], Chia-Lin Chou[2,8*] and Hong-Yue Lai[11,12,17*]

[1]Department of Pathology, Chi Mei Medical Center, [2]Department of Medical Technology, Chung Hwa University of Medical Technology, Tainan, [3]Institute of Biomedical Science, National Sun Yat-Sen University, Kaohsiung, [4]Department of Clinical Pathology, Chi Mei Medical Center, Tainan, [5]Department of Radiation Oncology, Chi Mei Medical Center, Liouying, [6]Department of Radiation Oncology, Chi Mei Medical Center, [7]Department of Pharmacy, Chia-Nan University of Pharmacy and Science, [8]Division of Colon and Rectal Surgery, Department of Surgery, Chi Mei Medical Center, [9]Division of Hematology and Oncology, Department of Internal Medicine, Chi-Mei Medical Center, [10]College of Pharmacy and Science, Chia Nan University, [11]Department of Medical Research, Chi Mei Medical Center, [12]Trans-Omic Laboratory for Precision Medicine, Precision Medicine Center, Chi Mei Medical Center, Tainan, [13]Department of Laboratory Medicine, China Medical University Hospital, Taichung, [14]Division of General Internal Medicine, Chi Mei Medical Center, [15]Department of Environment Engineering and Science, Chia Nan University of Pharmacy and Science, Tainan, [16]Institute of Precision Medicine, National Sun Yat-Sen University, Kaohsiung and [17]Department of Pharmacology, School of Medicine, College of Medicine, China Medical University, Taichung, Taiwan

*Chia-Lin Chou and Hong-Yue Lai contributed equally

Summary. Background. Concurrent chemoradiotherapy (CCRT) is suggested before resection surgery in the control of rectal cancer. Unfortunately, treatment outcomes are widely variable and highly patient-specific. Notably, rectal cancer patients with distant metastasis generally have a much lower survival rate. Accordingly, a better understanding of the genetic background of patient cohorts can aid in predicting CCRT efficacy and clinical outcomes for rectal cancer before distant metastasis.

Methods. A published transcriptome dataset (GSE35452) (n=46) was utilized to distinguish prospective genes concerning the response to CCRT. We recruited 172 rectal cancer patients, and the samples were collected during surgical resection after CCRT. Immunohistochemical (IHC) staining was performed to evaluate the expression level of regenerating family member 3 alpha (REG3A). Pearson's chi-squared test appraised the relevance of REG3A protein expression to clinicopathological parameters. The Kaplan-Meier method was utilized to generate survival curves, and the log-rank test was performed to compare the survival distributions between two given groups.

Results. Employing a transcriptome dataset (GSE35452) and focusing on the inflammatory response (GO: 0006954), we recognized that *REG3A* is the most significantly upregulated gene among CCRT non-responders (log2 ratio=1.2472, p=0.0079). Following IHC validation, high immunoexpression of REG3A was

Corresponding Author: Hong-Yue Lai, Ph.D., Department of Pharmacology, School of Medicine, College of Medicine, China Medical University, Taichung 404, Taiwan. e-mail: golddigger815@yahoo.com.tw and Chia-Lin Chou, M.D., Ph.D., Division of Colon and Rectal Surgery, Department of Surgery, Chi Mei Medical Center, Tainan 710, Taiwan. e-mail: clchou3@gmail.com

www.hh.um.es. DOI: 10.14670/HH-18-615

Abbreviations. ATP5F1A, ATP synthase F1 subunit alpha; ATP5F1B, ATP synthase F1 subunit beta; CCRT, concurrent chemoradiotherapy; CRC, colorectal cancer; DEFA5, defensin alpha 5; DEFA6, defensin alpha 6; DSS, disease-specific survival; ECM, extracellular matrix; EGFR, epidermal growth factor receptor; ERK1/2, extracellular signal-regulated kinases 1 and 2; FN1, fibronectin 1; IL6, interleukin 6; IL10, interleukin 10; IL17, interleukin 17; iNOS, inducible nitric oxide synthase; ITLN1, intelectin 1; ITLN2, intelectin 2; JAK2, Janus kinase 2; LRFS, local recurrence-free survival; MeFS, metastasis-free survival; NOS2, nitric oxide synthase 2; PI3Kγ, phosphoinositide 3-kinase gamma; REG3A, regenerating family member 3 alpha; STAT3, signal transducer and activator of transcription 3; TAM, tumor-associated macrophage, TGFβ, transforming growth factor beta; TLR3, toll-like receptor 3; TME, tumor microenvironment; TNFα, tumor necrosis factor alpha

considerably linked to advanced post-CCRT tumor status (p<0.001), post-CCRT lymph node metastasis (p=0.042), vascular invasion (p=0.028), and low-grade tumor regression (p=0.009). In the multivariate analysis, high immunoexpression of REG3A was independently correlated with poor disease-specific survival (DSS) (p=0.004) and metastasis-free survival (MeFS) (p=0.045). The results of the bioinformatic analysis also supported the idea that REG3A overexpression is implicated in rectal carcinogenesis.

Conclusion. In the current study, we demonstrated that REG3A overexpression is correlated with poor CCRT effectiveness and inferior patient survival in rectal cancer. The predictive and prognostic utility of REG3A expression may direct patient stratification and decision-making more accurately for those patients.

Key words: Rectal cancer, Chemoradiotherapy, *REG3A*, Inflammation, Lectin

Introduction

In 2020, colorectal cancer (CRC) was the third most common cancer and the second most deadly malignancy worldwide (Sung et al., 2021). Even though there is a general decline in CRC morbidity, this favorable trend masks the increasing incidence of rectal cancer, especially in generations younger than 50 years old (Xi and Xu, 2021). With advances in detailed pathological assessment and multimodality therapy, the management of rectal cancer keeps evolving. For rectal cancer patients with locally advanced disease, concurrent chemo-radiotherapy (CCRT) is suggested before resection surgery to diminish the risk of local recurrence (Keller et al., 2020). Unfortunately, treatment outcomes are widely variable and highly patient-specific. Additionally, the 5-year survival rate is 90% for rectal cancer patients diagnosed at a localized stage, whereas the 5-year survival rate is only 17% for those with distant metastasis, according to the Surveillance, Epidemiology, and End Results (SEER) database. Accordingly, a better understanding of the genetic background of patient cohorts can aid in predicting CCRT efficacy and clinical outcomes for rectal cancer before distant metastasis. With the involvement of genetic biomarkers for risk stratification and formulating the best treatment strategy, some patients may even eliminate the need for surgery and improve their quality of life.

The dynamic interplay of malignant cells with the tumor microenvironment (TME) made up of immune cells, fibroblasts, and the extracellular matrix (ECM) can determine CRC development and treatment responses (Binnewies et al., 2018). In proportion to the quantification of $CD3^+$/$CD8^+$ lymphocytes at the core of the tumor and at the tumor's edge (invasive margin), high Immunoscore has been suggested to be a stronger indicator than microsatellite instability for predicting favorable CRC patient survival (Mlecnik et al., 2016). In terms of macrophages, they generally can be divided into inflammatory (M1) and anti-inflammatory (M2) phenotypes. Although patients with inflammatory bowel disease are significantly associated with CRC development due to the neoplastic effects of chronic inflammation (Shah and Itzkowitz, 2022), rectal cancer with M2 macrophage-mediated immunosuppressive TME is correlated with CCRT resistance and distant metastasis (Kamran et al., 2019). Moreover, selective inhibition of macrophage phosphoinositide 3-kinase gamma (PI3Kγ) that promotes immune suppression can restore $CD8^+$ T cell cytotoxicity and improve antitumor immunity (Kaneda et al., 2016). These examinations indicate inflammation's intricate roles in tumor development and treatment efficacy that need to be delicately managed.

The human regenerating family member 3 alpha (*REG3A*) gene, mapped to chromosome 2p12, encodes a glycan-binding protein that preferentially recognizes and binds carbohydrate moieties protruding from glycoproteins. REG3A, also known as hepatocarcinoma-intestine-pancreas (HIP)/pancreatitis-associated protein (PAP), is a secreted calcium-dependent (C-type) lectin and is explicitly detected in the pancreas and intestine (Zhang et al., 2019). Also, REG3A mRNA has been detected at a high level in liver tumors but not observed in normal and nontumoral liver tissue (Lasserre et al., 1992). In response to inflammatory cytokine interleukin 6 (IL6), enhanced REG3A expression can trigger pancreatic cancer cell proliferation and tumorigenesis through the epidermal growth factor receptor (EGFR)/Janus kinase 2 (JAK2)/signal transducer and activator of transcription 3 (STAT3) signaling (Liu et al., 2015), suggesting that REG3A plays a critical role in inflammation-related pancreatic cancer. However, in skin injury, it has been indicated that IL17-induced REG3A can inhibit the release of toll-like receptor 3 (TLR3)-mediated inflammatory cytokines tumor necrosis factor alpha (TNFα) and IL6 to protect against impaired wound healing in diabetes (Wu et al., 2016), which may imply that REG3A has anti-inflammatory activities. Moreover, in infectious diseases, REG3A has been demonstrated to exhibit bactericidal activity against gram-positive bacteria by interacting with carbohydrate moieties (Cash et al., 2006) and attenuate inflammation in colitis via oxidative stress reduction (Darnaud et al., 2018). In addition, binding to fibronectin 1 (FN1), REG3A overexpression has been reported to promote cell proliferation through activating the AKT and extracellular signal-regulated kinases 1 and 2 (ERK1/2) pathways and correlated with CRC risk (Ye et al., 2016). Nevertheless, the correlations among inflammation, REG3A expression, CCRT efficacy, and patient survival in rectal cancer remain an open question.

Materials and methods

Analysis of differential gene expression in rectal cancer

Inclusive of forty-six rectal adenocarcinoma patients managed by preoperative CCRT, a transcriptome dataset

(GSE35452) was utilized to distinguish prospective genes concerning the response to CCRT. Tumor biopsies were gathered amid colonoscopic examination before undergoing neoadjuvant CCRT and were used for RNA extraction. The genome-scale platform Affymetrix GeneChip™ Human Genome Array was employed for transcriptome profiling, and all probesets were explored without preselection. The biopsies were separated into "resistance" and "sensitivity" by the response to CCRT, and a comparison between these two groups was performed under supervision. We performed differential gene expression analysis spotlighting the inflammatory response (GO: 0006954) and then picked out those genes with log2 ratio >0.2 or <-0.2 and $p<0.01$ for further investigation.

Patient recruitment and enrollment

The review and approval of this study were conducted by the Ethics Committee and Institutional Review Board (IRB) of Chi Mei Medical Center (IRB10302014). Retrieved from our biobank, the 172 FFPE tumor samples of consecutive rectal cancer patients diagnosed between 1998 and 2004 were examined. Before the surgical intervention, all patients received neoadjuvant CCRT, inclusive of a total dose of 45-50 Gy radiation therapy in twenty-five fractions across five weeks concurrent with a continuous 24 hour infusion of 5-FU-containing chemotherapy. For patients with node status beyond N1 or tumor status beyond T3, adjuvant chemotherapy was carried out before or after CCRT. The pathological and clinical features and patient survival were acquired by retrospectively reviewing the medical records. Primarily diagnosed with rectal cancer by colonoscopic examination, all patients had no distant metastasis as determined by chest X-ray and abdomino-pelvic computed tomography.

Histopathological evaluation and scoring of immunohisto-chemical staining

To avoid bias, the patients' clinical information was unknown to two independent pathologists (Tzu-Ju Chen and Wan-Shan Li) who evaluated all tumor samples. The criteria of cancer staging conformed to the eighth edition of the AJCC tumor-node-metastasis (TNM) staging system. A grading system for tumor regression evaluated by pathological features using surgical specimens was introduced to predict CCRT efficacy (Dworak et al., 1997). Immunohistochemical (IHC) staining was conducted as mentioned in our previous study (Chan et al., 2020). To melt the paraffin, the slides were put in a 65°C oven. After deparaffinized with xylene, the slides were gradually rehydrated using ethanol. Heat-induced epitope retrieval (HIER) was carried out using sodium citrate buffer (10 mM sodium citrate, pH 6) in a microwave for 20 min once the temperature had reached 98°C. Afterwards, the slides were subjected to REG3A primary antibody (PA5-23341, 1:100) (Thermo Fisher Scientific, Rockford, IL, USA) incubation at room temperature for 1h and then incubated with peroxidase-linked secondary antibody (Dako EnVision Detection System, Peroxidase/DAB) (Agilent Technologies, Santa Clara, CA, USA) at room temperature for 30 min. To quantify REG3A immunoexpression from the IHC image, the H-score was employed and generated referring to the following formulation: H-score=ΣPi (i+1), where Pi is the percentage (0% to 100%) of stained tumor cells for each intensity, and i is the intensity (0 to 3+) of staining. Accordingly, the H-score

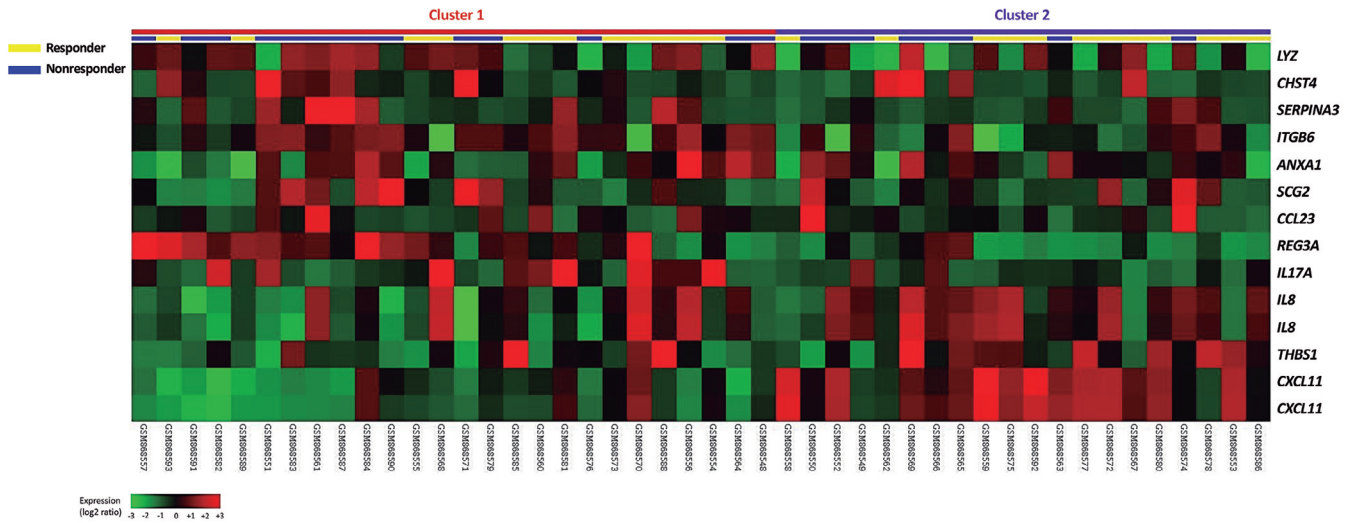

Fig. 1. Analysis of differential gene expression concerning inflammatory response and CCRT effectiveness in rectal cancer. The expression levels of upregulated and downregulated genes are marked in red and green, correspondingly. We distinguished *REG3A* as the most considerably upregulated gene relevant to the inflammatory response (GO: 0006954) among CCRT nonresponders.

Table 1. Profiling of differentially expressed genes concerning the inflammatory response (GO: 0006954) and CCRT effectiveness in rectal cancer.

Probe	Comparison Log Ratio	Comparison p-Value	Gene Symbol	Gene Name	Biological Process	Molecular Function
1555745_a_at	1.0541	0.0088	LYZ	Lysozyme (renal amyloidosis)	Cell wall catabolic process, cytolysis, defense response to bacterium, inflammatory response, metabolic process	Catalytic activity, hydrolase activity, acting on glycosyl bonds, lysozyme activity, protein binding
201012_at	0.4402	0.0035	ANXA1	Annexin A1	Anti-apoptosis, arachidonic acid secretion, cell cycle, cell motility, cell surface receptor linked signal transduction, inflammatory response, keratinocyte differentiation, lipid metabolic process, peptide cross-linking, regulation of cell proliferation, signal transduction	Calcium ion binding, calcium-dependent phospholipid binding, phospholipase A2 inhibitor activity, phospholipase inhibitor activity, phospholipid binding, protein binding, bridging, receptor binding, structural molecule activity
202376_at	0.7707	0.0031	SERPINA3	Serpin peptidase inhibitor; clade A (alpha-1 antiproteinase; antitrypsin); member 3	Acute-phase response, inflammatory response, regulation of lipid metabolic process	DNA binding, chymotrypsin inhibitor activity, endopeptidase inhibitor activity, protein binding, serine-type endopeptidase inhibitor activity
204035_at	0.6374	0.0004	SCG2	Secretogranin II (chromogranin C)	MAPKKK cascade, angiogenesis, cell motility, endothelial cell migration, eosinophil chemotaxis, induction of positive chemotaxis, inflammatory response, intracellular signaling cascade, negative regulation of apoptosis, negative regulation of endothelial cell proliferation, positive regulation of endothelial cell proliferation, protein secretion	Calcium ion binding, chemoattractant activity, cytokine activity
205815_at	1.2472	0.0079	REG3A	Regenerating islet-derived 3 alpha	Acute-phase response, cell proliferation, heterophilic cell adhesion, inflammatory response, multicellular organismal development	Sugar binding
210549_s_at	0.2255	0.0034	CCL23	Chemokine (C-C motif) ligand 23	G-protein coupled receptor protein signaling pathway, cell-cell signaling, cellular calcium ion homeostasis, chemotaxis, immune response, inflammatory response, negative regulation of cell proliferation, signal transduction	Chemokine activity, cytokine activity, heparin binding
220446_s_at	0.7544	0.0004	CHST4	Carbohydrate (N-acetylglucosamine 6-O) sulfotransferase 4	N-acetylglucosamine metabolic process, carbohydrate metabolic process, cell adhesion, cell motility, cell-cell signaling, immune response, inflammatory response, protein amino acid sulfation, sulfur metabolic process	N-acetylglucosamine 6-O-sulfotransferase activity, sulfotransferase activity, transferase activity
226535_at	0.747	0.0003	ITGB6	Integrin; beta 6	Cell adhesion, cell-matrix adhesion, inflammatory response, integrin-mediated signaling pathway, multicellular organismal development	Binding, integrin binding, protein binding, receptor activity
201107_s_at	-0.2892	0.0088	THBS1	Thrombospondin 1	Blood coagulation, cell adhesion, cell motility, inflammatory response, multicellular organismal development, negative regulation of angiogenesis, nervous system development	Calcium ion binding, endopeptidase inhibitor activity, heparin binding, protein binding, signal transducer activity, structural molecule activity
202859_x_at	-0.5296	0.0058	IL8	Interleukin 8	G-protein coupled receptor protein signaling pathway, angiogenesis, calcium-mediated signaling, cell adhesion, cell cycle arrest, cell motility, cell-cell signaling, chemotaxis, immune response, induction of positive chemotaxis, inflammatory response, intracellular signaling cascade, negative regulation of cell proliferation, neutrophil activation, neutrophil chemotaxis, regulation of cell adhesion, regulation of retroviral genome replication, signal transduction	Chemokine activity, cytokine activity, interleukin-8 receptor binding, protein binding
211506_s_at	-0.7158	0.0068	IL8	Interleukin 8	G-protein coupled receptor protein signaling pathway, angiogenesis, calcium-mediated signaling, cell adhesion, cell cycle arrest, cell motility, cell-cell signaling, chemotaxis, immune response, induction of positive chemotaxis, inflammatory response, intracellular signaling cascade, negative regulation of cell proliferation, neutrophil activation, neutrophil chemotaxis, regulation of cell adhesion, regulation of retroviral genome replication, signal transduction	Chemokine activity, cytokine activity, interleukin-8 receptor binding, protein binding
210163_at	-1.2994	<0.0001	CXCL11	Chemokine (C-X-C motif) ligand 11	Cell-cell signaling, chemotaxis, immune response, inflammatory response, signal transduction	Chemokine activity, cytokine activity
211122_s_at	-1.3734	0.0001	CXCL11	Chemokine (C-X-C motif) ligand 11	Cell-cell signaling, chemotaxis, immune response, inflammatory response, signal transduction	Chemokine activity, cytokine activity
216876_s_at	-0.5388	0.0043	IL17A	Interleukin 17A	Apoptosis, cell death, cell-cell signaling, immune response, inflammatory response, protein amino acid glycosylation	Cytokine activity

produced a value between 100 and 400 for each patient. To separate REG3A immunoreactivity into high and low levels, the median H-score of all scored cases was applied.

Statistical analysis

The SPSS statistical software version 20.0 was utilized for all data analyses. Pearson's chi-squared test appraised the relevance of REG3A expression to clinicopathological parameters. Three endpoints were assessed by a time interval between the operation and the development of events, including cancer death and first metastasis and local recurrence, to define survival. The Kaplan-Meier method was utilized to generate survival curves, and the log-rank test was performed to compare the survival distributions between two given groups. Integrating into parameters with prognostic value at the univariate level, a multivariate Cox proportional hazards model was employed to distinguish independent prognostic biomarkers. A two-tailed test with p less than 0.05 was considered statistically significant.

Results

REG3A is the most significantly upregulated gene relevant to CCRT resistance in rectal cancer patients

A transcriptome dataset (GSE35452), inclusive of rectal adenocarcinoma patients managed by preoperative CCRT (n=46), was utilized to distinguish prospective genes concerning the response to CCRT. Twenty-two (47.8%) and 24 (52.2%) tumor samples were considered resistant and sensitive, respectively, to CCRT, and a comparison between these two groups was performed to identify genetic biomarkers for predicting CCRT efficacy. To realize the role of inflammation in rectal cancer patients, we spotlighted the inflammatory response (GO: 0006954) and identified 14 probes covering 12 transcripts significantly relevant to the effectiveness of CCRT (Table 1, Fig. 1). Of these genes, *REG3A* was the most significantly upregulated gene among CCRT nonresponders (log2 ratio=1.2472, p=0.0079) and is explicitly detected in the intestine. This finding inspired us to further assess the predictive and prognostic impact of REG3A expression status in our rectal cancer cohort.

Clinicopathological characteristics of our rectal cancer cohort

Retrieved from our biobank, the 172 tissue blocks of rectal adenocarcinoma patients treated with preoperative CCRT were examined. Table 2 displays these patients' clinical and pathological characteristics and predicted CCRT efficacy. Eighty-one patients (47.1%) were primarily diagnosed with an early-stage disease (cT1-T2), and 125 patients (72.7%) had no metastatic lymph node (cN0) at first diagnosis. After completion of the preoperative CCRT, 86 surgical specimens (50%) showed invasion restricted to the muscularis propria (ypT1-T2), and 123 surgical specimens (71.5%) showed no metastatic lymph node (ypN0). Also, 15 (8.7%) and 5 (2.9%) surgical specimens presented vascular invasion and perineural invasion, correspondingly. Additionally, a grading system for tumor regression evaluated by pathological features was introduced to predict CCRT efficacy in rectal cancer patients, and the results revealed that 17 surgical specimens (9.9%) showed no tumor cells (total response) (grade 4).

Relationship between REG3A immunoexpression and clinicopathological characteristics

To correlate REG3A expression with clinicopathological characteristics and CCRT efficacy, IHC staining was carried out. As shown in Table 2, high immunoexpression of REG3A was considerably correlated with advanced tumor status (p<0.001), lymph node metastasis (p=0.042), and vascular invasion

Table 2. Relationship between REG3A expression and clinicopathological parameters in 172 rectal cancer patients treated with preoperative CCRT.

Parameter	No. of case	REG3A Expression		p-Value
		Low Exp.	High Exp.	
Gender				
Male	108	57	51	0.430
Female	64	29	35	
Age				
<70	106	56	50	0.347
≧70	66	30	36	
Pre-Tx tumor status (Pre-T)				
cT1-T2	81	42	39	0.760
cT3-T4	91	44	47	
Pre-Tx nodal status (Pre-N)				
cN0	125	65	60	0.494
cN1-N2	47	21	26	
Post-Tx tumor status (Post-T)				
ypT1-T2	86	55	31	<0.001*
ypT3-T4	86	31	55	
Post-Tx nodal status (Post-N)				
ypN0	123	68	55	0.042*
ypN1-N2	49	18	31	
Vascular invasion				
Absent	157	83	74	0.028*
Present	15	3	12	
Perineural invasion				
Absent	167	86	81	0.059
Present	5	0	5	
Tumor regression grade				
Grade 0-1	37	11	26	0.009*
Grade 2-3	118	63	55	
Grade 4	17	12	5	

Vascular invasion refers to lymphovascular invasion. Tx, treatment; *, statistically significant.

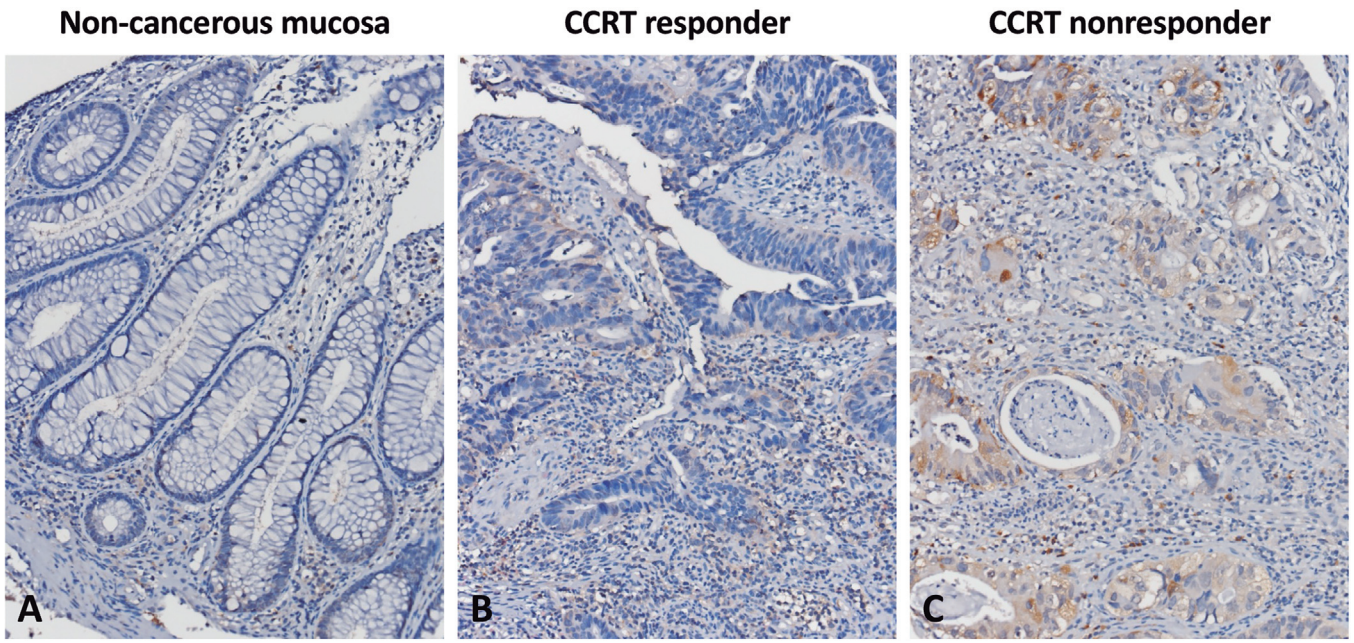

Fig. 2. Immunohistochemical detection of REG3A. The IHC staining showed predominantly cytoplasmic staining. **A.** Non-cancerous normal mucosa showed no REG3A immunoexpression. Rectal cancer resection samples exhibited low REG3A immunoexpression in patients responsive to CCRT and **(B)** high REG3A immunoexpression in patients nonresponsive to CCRT **(C)**. x 200.

Table 3. Univariate log-rank analysis for important clinicopathological variables and REG3A expression.

Parameter		No. of case	DSS		LRFS		MeFS	
			No. of event	p-Value	No. of event	p-Value	No. of event	p-Value
Gender	Male	108	20	0.9026	7	0.2250	17	0.3520
	Female	64	11		20		14	
Age	<70	106	19	0.8540	18	0.6615	20	0.7427
	≧70	66	12		9		11	
Pre-Tx tumor status (Pre-T)	cT1-T2	81	10	0.0776	10	0.2261	11	0.1745
	cT3-T4	91	21		17		20	
Pre-Tx nodal status (Pre-N)	cN0	125	19	0.0711	15	0.0070*	19	0.0973
	cN1-N2	47	21		12		12	
Post-Tx tumor status (Post-T)	ypT1-T2	86	7	0.0006*	7	0.0040*	8	0.0033*
	ypT3-T4	86	24		20		23	
Post-Tx nodal status (Post-N)	ypN0	123	21	0.5998	16	0.1320	20	0.4634
	ypN1-N2	49	10		11		11	
Vascular invasion	Absent	157	25	0.0184*	21	0.0028*	27	0.4470
	Present	15	6		6		4	
Perineural invasion	Absent	167	29	0.2559	25	0.0940	30	0.9083
	Present	5	2		2		1	
Tumor regression grade	Grade 0-1	37	13	0.0038*	10	0.0090*	14	0.0006*
	Grade 2-3	118	17		17		16	
	Grade 4	17	1		0		1	
REG3A expression	Low Exp.	86	9	<0.0001*	7	0.0011*	8	0.0015*
	High Exp.	86	22		20		23	

Vascular invasion refers to lymphovascular invasion. DSS, disease-specific survival; LRFS, local recurrence-free survival; MeFS, metastasis-free survival; *, statistically significant.

(p=0.028) following CCRT. In addition, high immunoexpression of REG3A was significantly connected to low-grade tumor regression (p=0.009). Of surgical specimens with no or little response to CCRT (grade 0-1, n=37), 26 surgical specimens (70.3%) showed high immunoexpression of REG3A. Furthermore, the results of IHC staining showed that REG3A immunoexpression was considerably higher among CCRT nonresponders (Fig. 2A-C).

The prognostic role of REG3A expression in rectal cancer patients

Table 3 exhibits that 27 (15.7%) and 31 (18%) patients developed local recurrence and metastasis, correspondingly, and that 31 patients (18%) died because of rectal cancer. To appraise the prognostic impact of clinicopathological characteristics and REG3A immunoexpression, three endpoints, metastasis-free survival (MeFS), local recurrence-free survival (LRFS), and disease-specific survival (DSS), were analyzed. In the univariate analysis, the results revealed that high immunoexpression of REG3A (DSS, p<0.0001; LRFS, p=0.0011; MeFS, p=0.0015) (Fig. 3A-C), advanced tumor status after CCRT (DSS, p=0.0006; LRFS, p=0.004; MeFS, p=0.0033), and low-grade tumor regression (DSS, p=0.0038; LRFS, p=0.009; MeFS, p=0.0006) were significantly adversely prognostic of all three endpoints. Besides, high immunoexpression of REG3A was independently correlated with poor DSS and MeFS (p=0.004 and p=0.045) at the multivariate level (Table 4).

Bioinformatic analysis and functional prediction of REG3A

Considering that REG3A has been suggested to have anti-inflammatory activities, we performed a gene coexpression examination to find out the unrevealed roles of REG3A in rectal carcinogenesis. Acquired from the colorectal adenocarcinoma dataset (n=594), the top 200 differentially expressed genes exhibiting positive relationship (Table 5) or negative relationship (Table 6) with REG3A were then used to execute functional

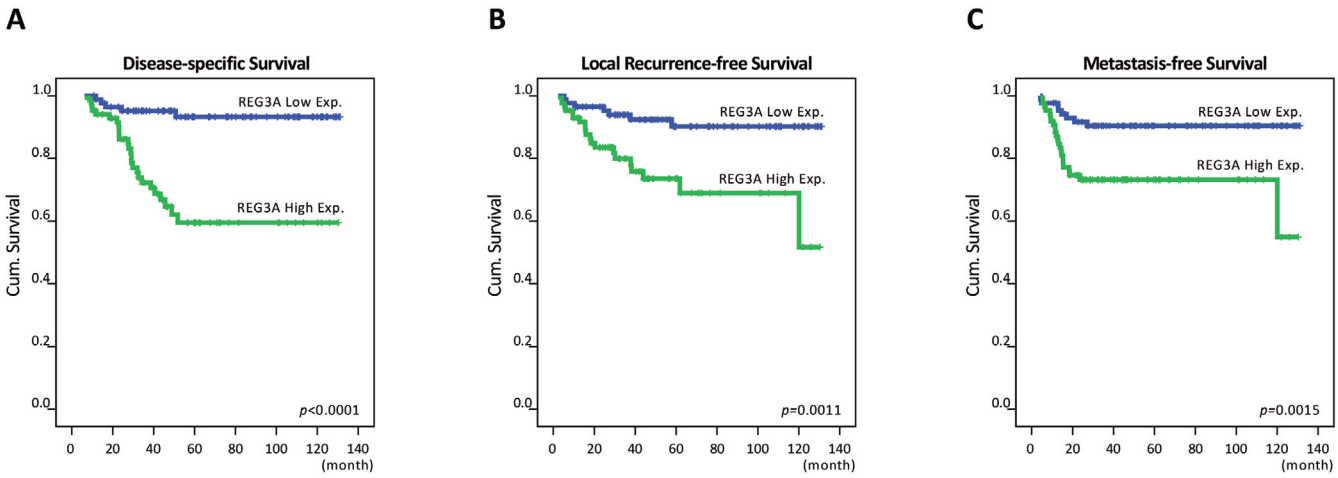

Fig. 3. Kaplan-Meier survival analysis. The Kaplan-Meier method with a log-rank test was performed, and the results revealed that high REG3A immunoexpression was notably connected with inferior disease-specific survival **(A)**, local recurrence-free survival **(B)** and metastasis-free survival **(C)**.

Table 4. Multivariate analysis.

Parameter	DSS			LRFS			MeFS		
	HR	95% CI	*p*-Value	HR	95% CI	*p*-Value	HR	95% CI	*p*-Value
Tumor regression grade	1.916	0.840-0.951	0.069	2.309	1.069-5.000	0.033*	2.278	1.139-4.545	0.020*
REG3A expression	4.436	1.624-12.114	0.004*	2.134	0.827-5.506	0.117	2.358	1.020-5.453	0.045*
Vascular invasion	1.968	0.804-4.814	0.138	1.653	0.642-4.256	0.298	-	-	-
Post-Tx tumor status (Post-T)	1.755	0.679-4.532	0.245	2.122	0.762-5.908	0.150	1.850	0.790-4.336	0.157
Pre-Tx nodal status (Pre-N)	-	-	-	1.938	0.833-4.506	0.125	-	-	-

Vascular invasion refers to lymphovascular invasion. DSS, disease-specific survival; LRFS, local recurrence-free survival; MeFS, metastasis-free survival; HR, hazard ratio; CI, confidence interval; *, statistically significant.

profiling applying the Gene Ontology (GO) database. In the context of biological processes (Fig. 4A), the most distinguished term co-upregulated with REG3A was modulation of process of another organism (GO: 0035821, fold enrichment: 22.22) that includes defensin alpha 5 (*DEFA5*), *DEFA6*, and nitric oxide synthase 2 (*NOS2*). Comprising intelectin 1 (*ITLN1*) and *ITLN2*, oligosaccharide binding (GO: 0070492, fold enrichment: 31.24) was the most prominent term co-upregulated with REG3A in the context of molecular functions (Fig. 4B). Especially the *REG1A*, *REG1B*, and *REG3G* genes were involved in both the GO terms mentioned above. Moreover, in the group of cellular components (Fig. 4C), the most notable GO term co-upregulated with *REG3A* was mitochondrial proton-transporting ATP synthase, catalytic core (GO: 0005754, fold enrichment: 99.98) that contains ATP synthase F1 subunit alpha (*ATP5F1A*) and *ATP5F1B*.

Discussion

Belonging to a group of secreted C-type lectins, the REG family comprises five members: REG1A, REG1B, REG3A, REG3G, and REG4 in humans (Parikh et al., 2012). Physiologically, REG3A is expressed in Paneth cells located in the small intestinal crypts, but it can be induced in response to infection and inflammation in the large intestine (Darnaud et al., 2018). REG3A and its murine ortholog Reg3g (66% sequence similarity) have been indicated to exhibit antimicrobial activities against Gram-positive bacteria and have anti-inflammatory activities (Cash et al., 2006). In addition, Reg3b (75.1% sequence similarity), another murine ortholog of REG3A, can kill Gram-negative bacteria by binding to carbohydrate moieties on lipopolysaccharide (LPS) (Miki et al., 2012). Transcriptional upregulation of REG3A has been observed in CRC with high colonization by Fusobacterium nucleatum (F. nucleatum) (Lennard et al., 2016), which is a Gram-negative oral anaerobe and can be detected in up to 45% of CRC tissues (Yamamura et al., 2017). It has been reported that F. nucleatum promotes CRC through activation of the Wnt/β-catenin signaling (Rubinstein et al., 2019), a key driver in the initiation and progression of CRC. Additionally, REG3A and REG1A are highly expressed in liver cancer with β-catenin mutations and are demonstrated to be downstream targets of the β-catenin signaling (Cavard et al., 2006). Accordingly, whether F. nucleatum promotes CRC development through the Wnt/β-catenin signaling and ensuing REG3A upregulation requires further examination.

Typically, the polarization of inflammatory (M1) and anti-inflammatory (M2) macrophages is delicately controlled to maintain the balance between inflammation and tissue regeneration. Nevertheless, in the tumor milieu, microenvironmental perturbations skew this balance and generate tumor-associated macrophages (TAMs) (high M2/M1 ratio) (Zhou et al., 2020). As a significant component of the TME, TAMs are featured by tissue repair and fibrosis, immunosuppression, and cytotoxic T cell inhibition and release of IL10 and transforming growth factor beta (TGFβ) (Lech and Anders, 2013; Wang et al., 2021a). REG3A has also been suggested to play critical roles in tissue regeneration and repair and anti-inflammation (Wang et al., 2022); therefore, we tried to link REG3A to rectal carcinogenesis and CCRT resistance through TAMs. It has been reported that, following experimental cardiac injury, M1 macrophages promote cardiomyocytes to produce Reg3b that could further facilitate the polarization of M2 macrophages (Zhou et al., 2018). This finding implies that REG3A production is regulated by inflammatory stimulation and functions as an anti-inflammatory molecule prone to tumor development. Additionally, in rectal cancer, CCRT nonresponders have been correlated with reduced cytotoxic T cell infiltration and a post-CCRT M2 macrophage phenotype (Kamran et al., 2019). Collectively, more insight into TAM activity will reveal the mechanisms by which REG3A promotes tumorigenesis and confers CCRT resistance in rectal cancer.

CRC development is a progressive multistage

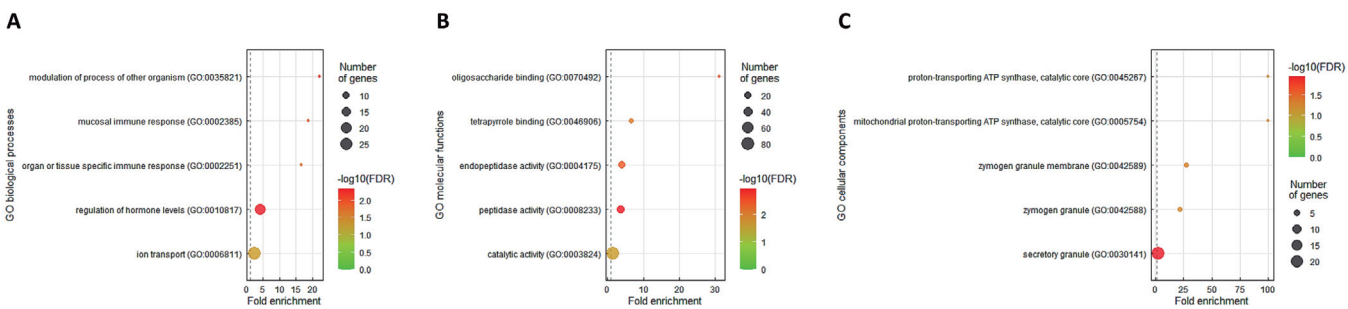

Fig. 4. The GO terms enriched in *REG3A* overexpression. The genes coexpressing with *REG3A* in the colorectal adenocarcinoma dataset (n=594) from The Cancer Genome Atlas (TCGA) database were acquired by making use of the cBioPortal online platform (http://cbioportal.org). The top 200 transcripts positively correlated with *REG3A* were then used for functional annotation applying the GO database (http://pantherdb.org) as determined by biological processes **(A)**, molecular functions **(B)**, or cellular components and ordered by fold enrichment **(C)**. An R script with a ggplot2 package was employed to visualize and present the critical GO terms.

Table 5. The top 200 genes positively correlated with REG3A.

Correlated Gene	Cytoband	Spearman's Correlation	p-Value	q-Value
REG1A	2p12	0.731	3.66E-100	7.27E-96
REG1B	2p12	0.666	3.71E-48	3.68E-44
DEFA5	8p23.1	0.5	8.80E-39	5.83E-35
SERPINA1	14q32.13	0.432	2.99E-28	1.49E-24
DEFA6	8p23.1	0.43	4.91E-28	1.95E-24
DMBT1	10q26.13	0.418	1.92E-26	6.36E-23
LCN2	9q34.11	0.409	2.95E-25	8.37E-22
REG3G	2p12	0.496	4.73E-24	1.17E-20
REG1CP	2p12	0.492	1.33E-23	2.94E-20
KLK12	19q13.41	0.394	2.07E-23	4.10E-20
ITLN2	1q23.3	0.371	1.05E-20	1.90E-17
SPINK4	9p13.3	0.368	1.82E-20	2.95E-17
KIAA1324	1p13.3	0.368	1.93E-20	2.95E-17
RAB26	16p13.3	0.367	2.89E-20	4.11E-17
KCNJ3	2q24.1	0.36	1.56E-19	2.06E-16
CLCA1	1p22.3	0.359	1.70E-19	2.06E-16
CA8	8q12.1	0.359	1.77E-19	2.06E-16
KLK3	19q13.33	0.359	2.11E-19	2.32E-16
L1TD1	1p31.3	0.353	9.02E-19	9.43E-16
SLC18A1	8p21.3	0.349	2.10E-18	2.09E-15
TRPA1	8q21.11	0.348	3.01E-18	2.85E-15
TOX	8q12.1	0.345	5.91E-18	5.34E-15
ATOH1	4q22.2	0.341	1.28E-17	1.06E-14
KIF19	17q25.1	0.341	1.43E-17	1.14E-14
OLFM4	13q14.3	0.34	1.77E-17	1.36E-14
RETNLB	3q13.13	0.339	2.16E-17	1.59E-14
HEPACAM2	7q21.2	0.336	4.10E-17	2.91E-14
GALNT8	12p13.32	0.334	6.39E-17	4.38E-14
ACPP	3q22.1	0.332	9.94E-17	6.59E-14
C4BPA	1q32.2	0.331	1.31E-16	8.40E-14
SLC28A3	9q21.32-q21.33	0.33	1.71E-16	1.06E-13
XBP1	22q12.1l22q12	0.329	1.99E-16	1.20E-13
TBX3	12q24.21	0.328	2.40E-16	1.40E-13
TCN1	11q12.1	0.326	4.19E-16	2.38E-13
FCGBP	19q13.2	0.324	5.62E-16	3.02E-13
ADH6	4q23	0.324	5.86E-16	3.07E-13
B3GNT6	11q13.5	0.324	6.86E-16	3.49E-13
FER1L6	8q24.13	0.323	8.16E-16	4.05E-13
MAP2K6	17q24.3	0.322	8.87E-16	4.30E-13
SLITRK6	13q31.1	0.322	9.25E-16	4.38E-13
NEURL1	10q24.33	0.32	1.57E-15	7.28E-13
CASP5	11q22.3	0.317	2.85E-15	1.29E-12
CFB	6p21.33	0.316	3.28E-15	1.45E-12
ASRGL1	11q12.3	0.313	6.57E-15	2.84E-12
DUOXA2	15q21.1	0.312	7.14E-15	3.02E-12
ZNF488	10q11.22	0.311	8.91E-15	3.69E-12
PLA2G4D	15q15.1	0.311	1.05E-14	4.28E-12
NOS2	17q11.2	0.307	2.16E-14	8.54E-12
PTGDR2	11q12.2	0.307	2.19E-14	8.54E-12
FYB2	1p32.2	0.307	2.36E-14	9.02E-12
DUOX2	15q21.1	0.306	2.49E-14	9.32E-12
SLC37A1	21q22.3	0.303	5.38E-14	1.94E-11
SP5	2q31.1	0.302	5.62E-14	2.00E-11
CYP4X1	1p33l1	0.302	6.30E-14	2.20E-11
CBLIF	11q12.1	0.301	7.52E-14	2.58E-11
ZBTB7C	18q21.1	0.299	1.12E-13	3.75E-11
COL9A2	1p34.2	0.299	1.15E-13	3.80E-11
LRG1	19p13.3	0.298	1.21E-13	3.93E-11
LRRC26	9q34.3	0.298	1.26E-13	4.02E-11
GAD1	2q31.1	0.297	1.59E-13	5.01E-11
REP15	12p11.22	0.294	2.70E-13	8.14E-11
BACE2	21q22.2-q22.3	0.294	3.02E-13	8.94E-11
MYO3B	2q31.1	0.293	3.81E-13	1.10E-10
PRSS1	7q34	0.29	5.79E-13	1.62E-10
MUC2	11p15.5	0.29	6.46E-13	1.78E-10
MB	22q12.3	0.29	6.69E-13	1.82E-10

Table 5. (Continued).

TMEM61	1p32.3	0.288	8.72E-13	2.33E-10
TNFSF13	17p13.1	0.288	8.80E-13	2.33E-10
ATP5F1A	18q21.1	0.288	9.85E-13	2.57E-10
MFSD2A	1p34.2	0.287	1.01E-12	2.62E-10
PRSS3P2	7q34	0.287	1.16E-12	2.92E-10
CNDP2	18q22.3	0.286	1.27E-12	3.15E-10
C4ORF19	4p14	0.286	1.37E-12	3.35E-10
MYRF	11q12.2	0.286	1.38E-12	3.35E-10
TRAF3IP2	6q21	0.285	1.57E-12	3.76E-10
FOXA3	19q13.32	0.285	1.73E-12	4.09E-10
CASP1	11q22.3	0.284	1.77E-12	4.14E-10
SBSPON	8q21.11	0.284	1.95E-12	4.50E-10
MEP1B	18q12.1	0.284	2.04E-12	4.66E-10
DLL1	6q27	0.282	3.02E-12	6.82E-10
DKK4	8p11.21	0.28	3.72E-12	8.12E-10
SERPINA3	14q32.13	0.28	4.30E-12	9.28E-10
H2AFY	5q31.1	0.277	6.89E-12	1.47E-09
KLK1	19q13.33	0.276	8.06E-12	1.69E-09
FUT2	19q13.33	0.275	9.05E-12	1.86E-09
KCNA6	12p13.32	0.275	9.12E-12	1.86E-09
SAMD5	6q24.3	0.275	9.19E-12	1.86E-09
ITLN1	1q23.3	0.274	1.18E-11	2.35E-09
MLEC	12q24.31	0.273	1.46E-11	2.85E-09
ZC3H12A	1p34.3	0.272	1.74E-11	3.23E-09
MISP3	19p13.12	0.272	1.76E-11	3.24E-09
SLC39A8	4q24	0.272	1.82E-11	3.31E-09
DEGS2	14q32.2	0.271	2.00E-11	3.62E-09
SAA2	11p15.1	0.27	2.44E-11	4.32E-09
ANO7	2q37.3	0.27	2.54E-11	4.46E-09
RFX6	6q22.1	0.338	3.26E-11	5.68E-09
P4HB	17q25.3	0.266	4.40E-11	7.47E-09
SSTR1	14q21.1	0.266	4.85E-11	8.17E-09
REG4	1p12	0.266	5.01E-11	8.36E-09
GFI1	1p22.1	0.265	5.30E-11	8.78E-09
GPR37	7q31.33	0.265	5.40E-11	8.86E-09
COL4A6	Xq22.3	0.265	5.49E-11	8.94E-09
MPDU1	17p13.1	0.265	5.58E-11	9.02E-09
CES3	16q22.1	0.264	6.45E-11	1.02E-08
RAP1GAP	1p36.12	0.264	6.48E-11	1.02E-08
RNF183	9q32	0.262	8.90E-11	1.36E-08
SCGB2A1	11q12.3	0.262	9.86E-11	1.48E-08
CYB5A	18q22.3	0.262	9.87E-11	1.48E-08
MAN1A1	6q22.31	0.262	1.00E-10	1.48E-08
SLC12A2	5q23.3	0.261	1.04E-10	1.53E-08
IL17C	16q24.2	0.261	1.10E-10	1.60E-08
HYAL1	3p21.31	0.261	1.13E-10	1.61E-08
CLRN3	10q26.2	0.261	1.13E-10	1.61E-08
SPDEF	6p21.31	0.261	1.14E-10	1.61E-08
CLDN2	Xq22.3	0.26	1.29E-10	1.77E-08
COL4A5	Xq22.3	0.26	1.30E-10	1.77E-08
MARC1	1q41	0.26	1.31E-10	1.78E-08
TRIM40	6p22.1	0.259	1.71E-10	2.18E-08
C4BPB	1q32.1	0.257	2.06E-10	2.54E-08
TRIM15	6p22.1	0.257	2.25E-10	2.73E-08
WNT4	1p36.12	0.257	2.31E-10	2.78E-08
PLA2G4A	1q31.1	0.257	2.35E-10	2.81E-08
AQP3	9p13.3	0.256	2.62E-10	3.12E-08
DUOXA1	15q21.1	0.256	2.69E-10	3.16E-08
PCCB	3q22.3	0.256	2.78E-10	3.23E-08
CCDC60	12q24.23	0.255	2.90E-10	3.34E-08
BIK	22q13.2	0.255	3.28E-10	3.75E-08
FDFT1	8p23.1	0.254	3.45E-10	3.90E-08
MOCOS	18q12.2	0.254	3.49E-10	3.92E-08
MUC1	1q22	0.253	4.02E-10	4.38E-08
KLK15	19q13.33	0.253	4.43E-10	4.81E-08
UGDH	4p14	0.253	4.55E-10	4.92E-08
PIGR	1q32.1	0.252	4.76E-10	5.12E-08
DUOX1	15q21.1	0.251	5.71E-10	6.00E-08

Table 5. (Continued).

UGT8	4q26	0.251	5.84E-10	6.11E-08
USP3	15q22.31	0.25	6.58E-10	6.81E-08
C17ORF78	17q12	0.249	7.60E-10	7.78E-08
KREMEN1	22q12.1	0.249	7.98E-10	8.14E-08
PLA2G3	22q12.2	0.249	8.50E-10	8.48E-08
WARS2	1p12	0.248	9.34E-10	9.09E-08
NRAP	10q25.3	0.248	9.52E-10	9.22E-08
CTSE	1q32.1	0.247	1.04E-09	9.97E-08
NAT1	8p22	0.247	1.14E-09	1.07E-07
AACS	12q24.31	0.246	1.24E-09	1.14E-07
SHC2	19p13.3	0.246	1.27E-09	1.16E-07
RASD1	17p11.2	0.246	1.30E-09	1.18E-07
SORD	15q21.1	0.246	1.39E-09	1.26E-07
SERPINB1	6p25.2	0.245	1.43E-09	1.28E-07
FOXI1	5q35.1	0.245	1.62E-09	1.43E-07
SPINK1	5q32	0.245	1.64E-09	1.44E-07
TMED6	16q22.1	0.245	1.65E-09	1.45E-07
GADD45G	9q22.2	0.244	1.76E-09	1.52E-07
GMDS	6p25.3	0.244	1.76E-09	1.52E-07
TMC5	16p12.3	0.244	1.86E-09	1.59E-07
LINC01124	2q31.1	0.244	1.87E-09	1.59E-07
NKX2-2	20p11.22	0.244	1.88E-09	1.60E-07
BMPER	7p14.3	0.243	1.98E-09	1.64E-07
GP2	16p12.3	0.243	2.02E-09	1.66E-07
FFAR2	19q13.12	0.243	2.02E-09	1.66E-07
UGT2B4	4q13.3	0.307	2.07E-09	1.69E-07
CATSPERB	14q32.12	0.243	2.18E-09	1.76E-07
CLCA2	1p22.3	0.241	2.75E-09	2.12E-07
PLPPR1	9q31.1	0.241	3.00E-09	2.28E-07
RPL17	18q21.1	0.24	3.23E-09	2.42E-07
FAM167A	8p23.1	0.239	3.70E-09	2.68E-07
AKR1C4	10p15.1	0.239	3.95E-09	2.85E-07
SEC11C	18q21.32	0.239	4.09E-09	2.91E-07
TC2N	14q32.12	0.238	4.37E-09	3.09E-07
SSR2	1q22	0.238	4.56E-09	3.18E-07
ENTPD8	9q34.3	0.238	4.77E-09	3.31E-07
HSD17B4	5q23.1	0.238	4.86E-09	3.34E-07
RPLP0	12q24.23	0.238	4.86E-09	3.34E-07
NFKBIZ	3q12.3	0.237	5.39E-09	3.61E-07
CBFA2T3	16q24.3	0.236	5.77E-09	3.85E-07
MTNR1A	4q35.2	0.236	5.79E-09	3.85E-07
CYB561D2	3p21.31	0.236	5.82E-09	3.86E-07
TXN2	22q12.3	0.236	6.28E-09	4.09E-07
DYRK4	12p13.32	0.235	7.36E-09	4.67E-07
TRIM16	17p12	0.234	7.73E-09	4.86E-07
CD5	11q12.2	0.234	8.00E-09	5.00E-07
ST6GALNAC1	17q25.1	0.234	8.20E-09	5.11E-07
MRPL16	11q12.1	0.234	8.26E-09	5.13E-07
ABCA12	2q35	0.234	8.64E-09	5.32E-07
DANCR	4q12	0.233	9.13E-09	5.55E-07
FBXO16	8p21.1	0.233	9.17E-09	5.56E-07
NDUFA9	12p13.32	0.233	9.75E-09	5.83E-07
PIM3	22q13.33	0.232	1.04E-08	6.21E-07
PITX1	5q31.1	0.232	1.12E-08	6.46E-07
ATP5F1B	12q13.3	0.231	1.25E-08	7.09E-07
ABHD3	18q11.2	0.231	1.27E-08	7.15E-07
PDE11A	2q31.2	0.231	1.29E-08	7.27E-07
USH1C	11p15.1	0.231	1.36E-08	7.63E-07
RGMB	5q15	0.231	1.39E-08	7.78E-07
CPS1	2q34	0.23	1.48E-08	8.19E-07
GSKIP	14q32.2	0.23	1.49E-08	8.20E-07
TEX101	19q13.31	0.23	1.59E-08	8.65E-07
EIF3L	22q13.1	0.23	1.60E-08	8.70E-07
ALDH3A2	17p11.2	0.229	1.65E-08	8.93E-07
SAMM50	22q13.31	0.229	1.68E-08	9.06E-07
CAPN9	1q42.2	0.229	1.69E-08	9.10E-07

Table 6. The top 200 genes negatively correlated with REG3A.

Correlated Gene	Cytoband	Spearman's Correlation	p-Value	q-Value
TRPC1	3q23	-0.344	6.74E-18	5.83E-15
FOXO1	13q14.11	-0.325	4.86E-16	2.68E-13
CACNG4	17q24.2	-0.306	2.93E-14	1.08E-11
CYTH3	7p22.1	-0.297	1.73E-13	5.36E-11
PPP1R3F	Xp11.23	-0.295	2.40E-13	7.33E-11
RGS9BP	19q13.11	-0.293	3.78E-13	1.10E-10
TIMP3	22q12.3	-0.292	4.01E-13	1.14E-10
CALB2	16q22.2	-0.287	1.05E-12	2.68E-10
WWC2	4q35.1	-0.281	3.12E-12	6.97E-10
HERPUD2	7p14.2	-0.281	3.29E-12	7.26E-10
SOGA3	6q22.33	-0.276	7.87E-12	1.66E-09
COMP	19p13.11	-0.274	1.10E-11	2.22E-09
MET	7q31.2	-0.273	1.31E-11	2.58E-09
TM4SF1	3q25.1	-0.273	1.49E-11	2.87E-09
FAM219A	9p13.3	-0.272	1.65E-11	3.16E-09
NDRG4	16q21	-0.272	1.72E-11	3.23E-09
RHCG	15q26.1	-0.272	1.73E-11	3.23E-09
PBX3	9q33.3	-0.27	2.38E-11	4.26E-09
HAND2	4q34.1	-0.267	3.78E-11	6.54E-09
CDK13	7p14.1	-0.267	4.08E-11	6.99E-09
CAP2	6p22.3	-0.265	5.80E-11	9.30E-09
RAB22A	20q13.32	-0.264	6.66E-11	1.04E-08
AHNAK2	14q32.33	-0.264	7.10E-11	1.09E-08
NKX3-2	4p15.33	-0.264	7.11E-11	1.09E-08
THBS4	5q14.1	-0.262	1.00E-10	1.48E-08
HERC5	4q22.1	-0.261	1.07E-10	1.57E-08
SCRN1	7p14.3	-0.261	1.12E-10	1.61E-08
CASC15	6p22.3	-0.261	1.18E-10	1.64E-08
HDGFL3	15q25.2	-0.261	1.18E-10	1.64E-08
USP27X	Xp11.23	-0.26	1.26E-10	1.74E-08
KBTBD2	7p14.3	-0.26	1.42E-10	1.90E-08
PHACTR3	20q13.32-q13.33	-0.259	1.45E-10	1.94E-08
FABP3	1p35.2	-0.259	1.51E-10	2.00E-08
PRDM6	5q23.2	-0.259	1.52E-10	2.00E-08
COL10A1	6q22.1	-0.259	1.57E-10	2.06E-08
SMIM10	Xq26.3	-0.259	1.69E-10	2.18E-08
FNBP1	9q34.11	-0.259	1.69E-10	2.18E-08
ST6GAL1	3q27.3	-0.259	1.71E-10	2.18E-08
NMT2	10p13	-0.258	1.85E-10	2.34E-08
PPP1R3D	20q13.33	-0.258	1.95E-10	2.45E-08
RAB3IL1	11q12.2-q12.3	-0.258	1.98E-10	2.47E-08
LRP11	6q25.1	-0.257	2.03E-10	2.52E-08
ZNF853	7p22.1	-0.257	2.10E-10	2.58E-08
GRP	18q21.32	-0.257	2.13E-10	2.59E-08
AMOTL2	3q22.2	-0.256	2.67E-10	3.16E-08
SATB2	2q33.1	-0.256	2.76E-10	3.23E-08
PALM	19p13.3	-0.255	3.27E-10	3.75E-08
SCHIP1	3q25.32-q25.33	-0.254	3.38E-10	3.84E-08
ITGB5	3q21.2	-0.254	3.54E-10	3.93E-08
OMD	9q22.31	-0.254	3.54E-10	3.93E-08
ASAP1	8q24.21-q24.22	-0.254	3.75E-10	4.14E-08
ADCY2	5p15.31	-0.254	3.82E-10	4.19E-08
SUN1	7p22.3	-0.252	4.98E-10	5.32E-08
UCHL1	4p13	-0.252	5.02E-10	5.34E-08
NCAM2	21q21.1	-0.251	5.66E-10	5.98E-08
FAXC	6q16.2	-0.251	5.98E-10	6.22E-08
WASF3	13q12.13	-0.25	7.04E-10	7.25E-08
SFRP4	7p14.1	-0.249	8.20E-10	8.31E-08
AQP1	7p14.3	-0.249	8.25E-10	8.32E-08
NCOA3	20q13.12	-0.249	8.41E-10	8.44E-08
ASPN	9q22.31	-0.249	8.68E-10	8.62E-08
ABTB2	11p13	-0.248	8.80E-10	8.68E-08
HSPBAP1	3q21.1	-0.248	8.82E-10	8.68E-08
PACS1	11q13.1-q13.2	-0.248	8.91E-10	8.72E-08
THRB	3p24.2	-0.247	1.04E-09	9.97E-08
JHY	11q24.1	-0.247	1.07E-09	1.02E-07

Table 6. (Continued).

ASTE1	3q22.1	-0.247	1.08E-09	1.02E-07
SUGCT	7p14.1	-0.247	1.12E-09	1.06E-07
DENND2C	1p13.2	-0.247	1.17E-09	1.10E-07
MPP2	17q21.31	-0.247	1.19E-09	1.11E-07
MYOZ3	5q33.1	-0.247	1.19E-09	1.11E-07
MYBL1	8q13.1	-0.246	1.26E-09	1.16E-07
AKAP12	6q25.1	-0.245	1.42E-09	1.28E-07
ZNFX1	20q13.13	-0.245	1.43E-09	1.28E-07
MPP6	7p15.3	-0.245	1.53E-09	1.36E-07
NPR3	5p13.3	-0.245	1.63E-09	1.44E-07
RAI14	5p13.2	-0.244	1.67E-09	1.45E-07
LINC01096	4p15.33	-0.244	1.84E-09	1.58E-07
SNX21	20q13.12	-0.244	1.89E-09	1.60E-07
CMTM7	3p22.3	-0.244	1.91E-09	1.60E-07
TTC7B	14q32.11	-0.244	1.91E-09	1.60E-07
CSNK2A2	16q21	-0.244	1.93E-09	1.61E-07
NOX4	11q14.3	-0.243	1.95E-09	1.62E-07
LRRC4C	11p12	-0.243	2.08E-09	1.69E-07
AAK1	2p13.3	-0.243	2.16E-09	1.75E-07
PCDH9	13q21.32	-0.242	2.29E-09	1.84E-07
USP42	7p22.1	-0.242	2.35E-09	1.88E-07
ISM1	20p12.1	-0.242	2.40E-09	1.92E-07
SPSB1	1p36.22	-0.242	2.60E-09	2.06E-07
RNF216	7p22.1	-0.242	2.61E-09	2.06E-07
EGFR	7p11.2	-0.242	2.62E-09	2.06E-07
MAML2	11q21	-0.242	2.62E-09	2.06E-07
MED29	19q13.2	-0.241	2.66E-09	2.08E-07
CRLF1	19p13.11	-0.241	2.68E-09	2.09E-07
ARHGEF25	12q13.3	-0.241	2.70E-09	2.09E-07
ZNF12	7p22.1	-0.241	2.70E-09	2.09E-07
SPAG9	17q21.33	-0.241	2.78E-09	2.13E-07
HSPB6	19q13.12	-0.241	2.94E-09	2.25E-07
ST6GAL2	2q12.3	-0.241	3.03E-09	2.30E-07
NEXN	1p31.1	-0.241	3.08E-09	2.33E-07
SPOCK1	5q31.2	-0.24	3.10E-09	2.33E-07
MOSPD1	Xq26.3	-0.24	3.27E-09	2.44E-07
PEA15	1q23.2	-0.24	3.36E-09	2.50E-07
FBXO17	19q13.2	-0.24	3.42E-09	2.53E-07
RIPOR1	16q22.1	-0.24	3.44E-09	2.53E-07
APBB1	11p15.4	-0.24	3.44E-09	2.53E-07
TNS1	2q35	-0.24	3.45E-09	2.53E-07
C7ORF25	7p14.1	-0.24	3.46E-09	2.53E-07
LRRN2	1q32.1	-0.239	3.66E-09	2.66E-07
HDAC5	17q21.31	-0.239	3.97E-09	2.86E-07
ENPP1	6q23.2	-0.239	3.98E-09	2.86E-07
PKD2	4q22.1	-0.239	4.01E-09	2.87E-07
NORAD	20q11.23	-0.238	4.24E-09	3.01E-07
AKT3	1q43-q44	-0.238	4.38E-09	3.09E-07
SORBS1	10q24.1	-0.238	4.50E-09	3.16E-07
TMEM185A	Xq28	-0.238	4.51E-09	3.16E-07
EPYC	12q21.33	-0.238	4.81E-09	3.33E-07
CDIPT	16p11.2	-0.237	4.95E-09	3.39E-07
ZCCHC24	10q22.3	-0.237	5.01E-09	3.42E-07
ZNF623	8q24.3	-0.237	5.10E-09	3.46E-07
GPSM1	9q34.3	-0.237	5.11E-09	3.46E-07
PIK3CA	3q26.32	-0.237	5.12E-09	3.46E-07
KATNAL1	13q12.3	-0.237	5.24E-09	3.53E-07
MOSMO	16p12.2	-0.237	5.58E-09	3.73E-07
COL11A1	1p21.1	-0.236	5.89E-09	3.89E-07
WDR53	3q29	-0.236	6.13E-09	4.02E-07
OGA	10q24.32	-0.236	6.14E-09	4.02E-07
IFIT1	10q23.31	-0.236	6.15E-09	4.02E-07
MMP11	22q11.23	-0.236	6.56E-09	4.26E-07
ZNF217	20q13.2	-0.235	6.66E-09	4.31E-07
NCS1	9q34.11	-0.235	6.89E-09	4.44E-07
SEPTIN7	7p14.2	-0.235	7.06E-09	4.54E-07
PSD	10q24.32	-0.235	7.16E-09	4.59E-07
GLIS2	16p13.3	-0.235	7.27E-09	4.64E-07

Table 6. (Continued).

IDS	Xq28	-0.235	7.29E-09	4.64E-07
SHISA4	1q32.1	-0.235	7.59E-09	4.80E-07
STK4	20q13.12	-0.235	7.69E-09	4.85E-07
HAND2-AS1	4q34.1	-0.234	7.93E-09	4.97E-07
TPD52L2	20q13.33	-0.234	8.59E-09	5.31E-07
TRIM9	14q22.1	-0.234	8.61E-09	5.31E-07
BLCAP	20q11.23	-0.234	8.93E-09	5.47E-07
GPM6B	Xp22.2	-0.234	8.94E-09	5.47E-07
SAMD4A	14q22.2	-0.233	9.08E-09	5.54E-07
MANCR	10p15.1	-0.233	9.44E-09	5.70E-07
MYLK4	6p25.2	-0.233	9.47E-09	5.70E-07
SYCP2	20q13.33	-0.233	9.62E-09	5.77E-07
RB1CC1	8q11.23	-0.233	9.86E-09	5.88E-07
SCRG1	4q34.1	-0.232	1.05E-08	6.22E-07
NCOA6	20q11.22	-0.232	1.06E-08	6.23E-07
NAP1L3	Xq21.32	-0.232	1.06E-08	6.23E-07
ISLR	15q24.1	-0.232	1.09E-08	6.41E-07
AGTR1	3q24	-0.232	1.10E-08	6.43E-07
TMEM240	1p36.33	-0.232	1.10E-08	6.43E-07
WDFY1	2q36.1	-0.232	1.10E-08	6.43E-07
DNTTIP1	20q13.12	-0.232	1.11E-08	6.44E-07
SSC5D	19q13.42	-0.232	1.11E-08	6.45E-07
FAM228B	2p23.3	-0.232	1.12E-08	6.46E-07
USP27X-AS1	Xp11.23	-0.232	1.18E-08	6.76E-07
NTM	11q25	-0.231	1.21E-08	6.95E-07
TMEM52B	12p13.2	-0.231	1.22E-08	6.96E-07
HSF2BP	21q22.3	-0.231	1.23E-08	7.00E-07
LAMP5	20p12.2	-0.231	1.27E-08	7.15E-07
MYL9	20q11.23	-0.231	1.35E-08	7.57E-07
ZNF251	8q24.3	-0.23	1.41E-08	7.85E-07
PNMA8B	19q13.32	-0.23	1.46E-08	8.08E-07
COL8A2	1p34.3	-0.23	1.51E-08	8.29E-07
GLCCI1	7p21.3	-0.23	1.54E-08	8.44E-07
ZNF347	19q13.42	-0.23	1.56E-08	8.54E-07
PRELP	1q32.1	-0.23	1.57E-08	8.59E-07
IL2RG	Xq13.1	-0.229	1.63E-08	8.84E-07
TMEM200B	1p35.3	-0.229	1.71E-08	9.14E-07
RBMS1	2q24.2	-0.229	1.73E-08	9.21E-07
WIPI2	7p22.1	-0.229	1.84E-08	9.76E-07
CTSV	9q22.33	-0.229	1.88E-08	9.94E-07
SDC4	20q13.12	-0.228	2.02E-08	1.06E-06
SULF2	20q13.12	-0.228	2.03E-08	1.06E-06
CILP2	19p13.11	-0.228	2.05E-08	1.07E-06
KCTD7	7q11.21	-0.228	2.12E-08	1.10E-06
IRAK2	3p25.3	-0.227	2.28E-08	1.17E-06
KLHL7	7p15.3	-0.227	2.28E-08	1.17E-06
RALGAPB	20q11.23	-0.227	2.31E-08	1.18E-06
ARHGAP42	11q22.1	-0.227	2.32E-08	1.18E-06
RDX	11q22.3	-0.227	2.40E-08	1.22E-06
INPP5F	10q26.11	-0.227	2.49E-08	1.25E-06
SFRP2	4q31.3	-0.227	2.52E-08	1.26E-06
PMEPA1	20q13.31	-0.227	2.52E-08	1.26E-06
BCL2L1	20q11.21	-0.226	2.52E-08	1.26E-06
MITF	3p13	-0.226	2.61E-08	1.30E-06
USP31	16p12.2	-0.226	2.67E-08	1.33E-06
COX19	7p22.3	-0.226	2.68E-08	1.33E-06
ACHE	7q22.1	-0.226	2.73E-08	1.35E-06
OTOA	16p12.2l16p12.2	-0.226	2.76E-08	1.36E-06
ZBTB10	8q21.13	-0.226	2.78E-08	1.37E-06
TUB	11p15.4	-0.225	2.93E-08	1.44E-06
C6ORF141	6p12.3	-0.225	2.97E-08	1.45E-06
CTNNBL1	20q11.23	-0.225	2.97E-08	1.45E-06
NUDCD3	7p13	-0.225	3.05E-08	1.48E-06
TAX1BP1	7p15.2	-0.225	3.10E-08	1.50E-06
DYNLRB1	20q11.22	-0.225	3.15E-08	1.52E-06
EREG	4q13.3	-0.225	3.20E-08	1.53E-06

process involving multiple genes, which is featured by heterogeneous outcomes and therapy responses. To assist patient stratification and therapeutic decision-making, a classification system encompassing tumor genomic, transcriptomic, and epigenomic subtypes and stromal and immune components has been proposed in CRC. This system comprises 4 consensus molecular subtypes (CMS1-4) with distinctive characterization: CMS1 (microsatellite unstable, 14%), CMS2 (canonical, 37%), CMS3 (metabolic, 13%), and CMS4 (mesenchymal, 23%) (Guinney et al., 2015). More specifically, among these molecular subtypes, two (CMS1 and CMS4) highly express immune-specific genes, which can reflect the extent and phenotype of immune infiltrates (Becht et al., 2016). The CMS1 subgroup is characterized by hypermutation rates and strong immune activation and is associated with a good prognosis. On the other hand, the CMS4 subgroup is featured by inflammation-triggered immunosuppressive cell infiltration (M2 macrophages and regulatory T cells), TGFβ and IL17 secretion, and chromosomal instability (CIN) and is correlated with poor prognosis (Dienstmann et al., 2017). As mentioned in the previous paragraph, REG3A can induce M2 macrophage polarization and create an immunosuppressive niche beneficial for tumor development. Additionally, in response to skin injury-mediated inflammation, the release of IL17 can exert anti-inflammatory activities through REG3A induction to prevent dysregulated inflammatory responses (Wu et al., 2016). Accordingly, REG3A overexpression is more specific to the CMS4 subgroup, which can add more value to guide treatment more precisely.

To find out the unrevealed functions of REG3A, we performed a gene coexpression analysis and found that many genes, including *DEFA5*, *DEFA6*, *NOS2*, *ITLN1*, *ITLN2*, *ATP5F1A*, and *ATP5F1B*, significantly co-upregulated with REG3A (Fig. 4) are implicated in rectal carcinogenesis. To maintain homeostasis between the host and the small intestinal microbial load, Paneth cells secrete several antimicrobial peptides, such as DEFA5, DEFA6, and REG3A (Bevins and Salzman, 2011). It has been indicated that high levels of DEFA5 and DEFA6 are indicators of colon adenoma formation (Nastase et al., 2011) and that high DEFA6 expression is an independent unfavorable prognosticator for CRC (Jeong et al., 2019). NOS2, also known as inducible nitric oxide synthase (iNOS), is responsible for the production of nitric oxide (NO) that has been suggested to play a role in immunosuppression and CRC progression (Porta et al., 2020). ITLN1, also known as omentin, is highly expressed in CRC and serves as a potential biomarker for CRC diagnosis and progression (Zhao et al., 2019), but the available studies on ITLN2 and tumor are restricted. Mitochondrial adenosine triphosphate (ATP) synthase produces most of the ATP that is essential for malignant tumor growth and emerges as a therapeutic target in cancer (Wang et al., 2021b). In CRC, it has been demonstrated that a high level of *ATP5F1A* is correlated with *TP53* mutations and CIN and may facilitate tumor development (Seth et al., 2009) and that *ATP5F1B* expression is highly detected in tumor tissue (Geyik et al., 2014). Altogether, these observations may support the idea that REG3A overexpression is a negative predictive and prognostic biomarker in rectal cancer.

Conclusion

In response to injury or infection, acute-phase proteins such as REG3A are released to resolve inflammation and avoid uncontrolled inflammatory responses. Nevertheless, prolonged high REG3A expression can create an immunosuppressive niche beneficial for tumor development. In the current study, we demonstrated that REG3A overexpression is correlated with poor CCRT effectiveness and inferior patient survival in rectal cancer. The predictive and prognostic utility of REG3A expression may direct patient stratification and decision-making more accurately for those patients.

Acknowledgements. The authors are grateful for the help from the Translational Research Laboratory at the Department of Medical Research of Chi Mei Medical Center in conducting this study.

Ethics approval. This study and its use of tumor samples that were de-identified from the biobank was approved by the Ethics Committee and Institutional Review Board of Chi Mei Medical Center (10302014) and followed the ethical guidelines of the Helsinki Declaration and the regulations of our government.

Consent to participate statement. As a rule, every participant signed informed consent before being enrolled in the biobank.

Availability of data and materials. The transcriptome dataset (GSE35452) analyzed in the current study is available in a published archive from the Gene Expression Omnibus (GEO) database (National Center for Biotechnology Information, Bethesda, MD, USA).

Authors' contributions. Conceptualization: C.-L. Chou and H.-Y. Lai; methodology: W.-S. Li, T.-J. Chen, S.-W. Lee, C.-C. Yang, Y.-F. Tian, Y.-H. Kuo, H.-H. Tsai, L.-C. Wu, C.-F. Yeh, and Y.-L. Shiue; investigation: W.-S. Li, T.-J. Chen, S.-W. Lee, C.-C. Yang, Y.-F. Tian, Y.-H. Kuo, H.-H. Tsai, L.-C. Wu, C.-F. Yeh, and Y.-L. Shiue; formal analysis: W.-S. Li, T.-J. Chen, S.-W. Lee, C.-C. Yang, Y.-F. Tian, Y.-H. Kuo, H.-H. Tsai, L.-C. Wu, C.-F. Yeh, and Y.-L. Shiue; resources: L.-C. Wu, C.-F. Yeh, and Y.-L. Shiue; validation: W.-S. Li, T.-J. Chen, S.-W. Lee, C.-C. Yang, Y.-F. Tian, Y.-H. Kuo, and H.-H. Tsai; visualization: W.-S. Li, T.-J. Chen, S.-W. Lee, C.-C. Yang, Y.-F. Tian, Y.-H. Kuo, and H.-H. Tsai; writing - original draft: C.-L. Chou and H.-Y. Lai; writing - review & editing: H.-Y. Lai; funding acquisition: C.-L. Chou; supervision: C.-L. Chou and H.-Y. Lai. All authors contributed to the article and approved the submitted version.

Conflict of interest. The authors declare that the research was conducted in the absence of any commercial or financial relationship that could be construed as a potential conflict of interest.

Funding. This research received no external funding.

References

Becht E., de Reyniès A., Giraldo N.A., Pilati C., Buttard B., Lacroix L., Selves J., Sautès-Fridman C., Laurent-Puig P. and Fridman W.H.

(2016). Immune and stromal classification of colorectal cancer is associated with molecular subtypes and relevant for precision immunotherapy. Clin. Cancer Res. 22, 4057-4066.

Bevins C.L. and Salzman N.H. (2011). Paneth cells, antimicrobial peptides and maintenance of intestinal homeostasis. Nat. Rev. Microbiol. 9, 356-368.

Binnewies M., Roberts E.W., Kersten K., Chan V., Fearon D.F., Merad M., Coussens L.M., Gabrilovich D.I., Ostrand-Rosenberg S., Hedrick C.C., Vonderheide R.H., Pittet M.J., Jain R.K., Zou W., Howcroft T.K., Woodhouse E.C., Weinberg R.A. and Krummel M.F. (2018). Understanding the tumor immune microenvironment (TIME) for effective therapy. Nat. Med. 24, 541-550.

Cash H.L., Whitham C.V., Behrendt C.L. and Hooper L.V. (2006). Symbiotic bacteria direct expression of an intestinal bactericidal lectin. Science 313, 1126-1130.

Cavard C., Terris B., Grimber G., Christa L., Audard V., Radenen-Bussiere B., Simon M.T., Renard C.A., Buendia M.A. and Perret C. (2006). Overexpression of regenerating islet-derived 1 alpha and 3 alpha genes in human primary liver tumors with beta-catenin mutations. Oncogene 25, 599-608.

Chan T.C., Wu W.J., Li W.M., Shiao M.S., Shiue Y.L. and Li C.F. (2020). SLC14A1 prevents oncometabolite accumulation and recruits HDAC1 to transrepress oncometabolite genes in urothelial carcinoma. Theranostics 10, 11775-11793.

Darnaud M., Dos Santos A., Gonzalez P., Augui S., Lacoste C., Desterke C., De Hertogh G., Valentino E., Braun E., Zheng J., Boisgard R., Neut C., Dubuquoy L., Chiappini F., Samuel D., Lepage P., Guerrieri F., Doré J., Bréchot C., Moniaux N. and Faivre J. (2018). Enteric delivery of regenerating family member 3 alpha alters the intestinal microbiota and controls inflammation in mice with colitis. Gastroenterology 154, 1009-1023.e1014.

Dienstmann R., Vermeulen L., Guinney J., Kopetz S., Tejpar S. and Tabernero J. (2017). Consensus molecular subtypes and the evolution of precision medicine in colorectal cancer. Nat. Rev. Cancer 17, 79-92.

Dworak O., Keilholz L. and Hoffmann A. (1997). Pathological features of rectal cancer after preoperative radiochemotherapy. Int. J. Colorectal Dis. 12, 19-23.

Geyik E., Igci Y.Z., Pala E., Suner A., Borazan E., Bozgeyik I., Bayraktar E., Bayraktar R., Ergun S., Cakmak E.A., Gokalp A. and Arslan A. (2014). Investigation of the association between ATP2B4 and ATP5B genes with colorectal cancer. Gene 540, 178-182.

Guinney J., Dienstmann R., Wang X., de Reyniès A., Schlicker A., Soneson C., Marisa L., Roepman P., Nyamundanda G., Angelino P., Bot B.M., Morris J.S., Simon I.M., Gerster S., Fessler E., De Sousa E.M.F., Missiaglia E., Ramay H., Barras D., Homicsko K., Maru D., Manyam G.C., Broom B., Boige V., Perez-Villamil B., Laderas T., Salazar R., Gray J.W., Hanahan D., Tabernero J., Bernards R., Friend S.H., Laurent-Puig P., Medema J.P., Sadanandam A., Wessels L., Delorenzi M., Kopetz S., Vermeulen L. and Tejpar S. (2015). The consensus molecular subtypes of colorectal cancer. Nat. Med. 21, 1350-1356.

Jeong D., Kim H., Kim D., Ban S., Oh S., Ji S., Kang D., Lee H., Ahn T.S., Kim H.J., Bae S.B., Lee M.S., Kim C.J., Kwon H.Y. and Baek M.J. (2019). Defensin alpha 6 (DEFA6) is a prognostic marker in colorectal cancer. Cancer Biomark. 24, 485-495.

Kamran S.C., Lennerz J.K., Margolis C.A., Liu D., Reardon B., Wankowicz S.A., Van Seventer E.E., Tracy A., Wo J.Y., Carter S.L., Willers H., Corcoran R.B., Hong T.S. and Van Allen E.M. (2019). Integrative molecular characterization of resistance to neoadjuvant chemoradiation in rectal cancer. Clin. Cancer Res. 25, 5561-5571.

Kaneda M.M., Messer K.S., Ralainirina N., Li H., Leem C.J., Gorjestani S., Woo G., Nguyen A.V., Figueiredo C.C., Foubert P., Schmid M.C., Pink M., Winkler D.G., Rausch M., Palombella V.J., Kutok J., McGovern K., Frazer K.A., Wu X., Karin M., Sasik R., Cohen E.E. and Varner J.A. (2016). PI3Kγ is a molecular switch that controls immune suppression. Nature 539, 437-442.

Keller D.S., Berho M., Perez R.O., Wexner S.D. and Chand M. (2020). The multidisciplinary management of rectal cancer. Natu. Rev. Gastroenterol. Hepatol. 17, 414-429.

Lasserre C., Christa L., Simon M.T., Vernier P. and Bréchot C. (1992). A novel gene (HIP) activated in human primary liver cancer. Cancer Res. 52, 5089-5095.

Lech M. and Anders H.J. (2013). Macrophages and fibrosis: How resident and infiltrating mononuclear phagocytes orchestrate all phases of tissue injury and repair. Biochim. Biophys. Acta 1832, 989-997.

Lennard K.S., Goosen R.W. and Blackburn J.M. (2016). Bacterially-associated transcriptional remodelling in a distinct genomic subtype of colorectal cancer provides a plausible molecular basis for disease development. PloS One 11, e0166282.

Liu X., Wang J., Wang H., Yin G., Liu Y., Lei X. and Xiang M. (2015). REG3A accelerates pancreatic cancer cell growth under IL-6-associated inflammatory condition: Involvement of a REG3A-JAK2/STAT3 positive feedback loop. Cancer Lett. 362, 45-60.

Miki T., Holst O. and Hardt W.D. (2012). The bactericidal activity of the C-type lectin RegIIIβ against Gram-negative bacteria involves binding to lipid A. J. Biol. Chem. 287, 34844-34855.

Mlecnik B., Bindea G., Angell H.K., Maby P., Angelova M., Tougeron D., Church S.E., Lafontaine L., Fischer M., Fredriksen T., Sasso M., Bilocq A.M., Kirilovsky A., Obenauf A.C., Hamieh M., Berger A., Bruneval P., Tuech J.J., Sabourin J.C., Le Pessot F., Mauillon J., Rafii A., Laurent-Puig P., Speicher M.R., Trajanoski Z., Michel P., Sesboüe R., Frebourg T., Pagès F., Valge-Archer V., Latouche J.B. and Galon J. (2016). Integrative analyses of colorectal cancer show immunoscore is a stronger predictor of patient survival than microsatellite instability. Immunity 44, 698-711.

Nastase A., Pâslaru L., Niculescu A.M., Ionescu M., Dumitraşcu T., Herlea V., Dima S., Gheorghe C., Lazar V. and Popescu I. (2011). Prognostic and predictive potential molecular biomarkers in colon cancer. Chirurgia (Bucur). 106, 177-185.

Parikh A., Stephan A.F. and Tzanakakis E.S. (2012). Regenerating proteins and their expression, regulation and signaling. Biomol. Concepts 3, 57-70.

Porta C., Consonni F.M., Morlacchi S., Sangaletti S., Bleve A., Totaro M.G., Larghi P., Rimoldi M., Tripodo C., Strauss L., Banfi S., Storto M., Pressiani T., Rimassa L., Tartari S., Ippolito A., Doni A., Soldà G., Duga S., Piccolo V., Ostuni R., Natoli G., Bronte V., Balzac F., Turco E., Hirsch E., Colombo M.P. and Sica A. (2020). Tumor-derived prostaglandin E2 promotes p50 NF-κB-dependent differentiation of monocytic MDSCs. Cancer Rese. 80, 2874-2888.

Rubinstein M.R., Baik J.E., Lagana S.M., Han R.P., Raab W.J., Sahoo D., Dalerba P., Wang T.C. and Han Y.W. (2019). Fusobacterium nucleatum promotes colorectal cancer by inducing Wnt/β-catenin modulator Annexin A1. EMBO Rep. 20, e47638.

Seth R., Keeley J., Abu-Ali G., Crook S., Jackson D. and Ilyas M. (2009). The putative tumour modifier gene ATP5A1 is not mutated in human colorectal cancer cell lines but expression levels correlate

with TP53 mutations and chromosomal instability. J. Clin. Pathol. 62, 598-603.

Shah S.C. and Itzkowitz S.H. (2022). Colorectal cancer in inflammatory bowel disease: Mechanisms and management. Gastroenterology 162, 715-730. e713.

Sung H., Ferlay J., Siegel R.L., Laversanne M., Soerjomataram I., Jemal A. and Bray F. (2021). Global cancer statistics 2020: GLOBOCAN estimates of incidence and mortality worldwide for 36 cancers in 185 countries. CA Cancer J. Clin. 71, 209-249.

Wang H., Yung M.M.H., Ngan H.Y.S., Chan K.K.L. and Chan D.W. (2021a). The impact of the tumor microenvironment on macrophage polarization in cancer metastatic progression. Int. J. Mol. Sci. 22, 6560.

Wang T., Ma F. and Qian H.L. (2021b). Defueling the cancer: ATP synthase as an emerging target in cancer therapy. Mol. Ther. Oncolytics 23, 82-95.

Wang L., Quan Y., Zhu Y., Xie X., Wang Z., Wang L., Wei X. and Che F. (2022). The regenerating protein 3A: A crucial molecular with dual roles in cancer. Mol. Biol. Rep. 49, 1491-1500.

Wu Y., Quan Y., Liu Y., Liu K., Li H., Jiang Z., Zhang T., Lei H., Radek K.A., Li D., Wang Z., Lu J., Wang W., Ji S., Xia Z. and Lai Y. (2016). Hyperglycaemia inhibits REG3A expression to exacerbate TLR3-mediated skin inflammation in diabetes. Nat. Commun. 7, 13393.

Xi Y. and Xu P. (2021). Global colorectal cancer burden in 2020 and projections to 2040. Transl. Oncol. 14, 101174.

Yamamura K., Baba Y., Miyake K., Nakamura K., Shigaki H., Mima K., Kurashige J., Ishimoto T., Iwatsuki M., Sakamoto Y., Yamashita Y., Yoshida N., Watanabe M. and Baba H. (2017). *Fusobacterium nucleatum* in gastroenterological cancer: Evaluation of measurement methods using quantitative polymerase chain reaction and a literature review. Oncol. Lett. 14, 6373-6378.

Ye Y., Xiao L., Wang S.J., Yue W., Yin Q.S., Sun M.Y., Xia W., Shao Z.Y. and Zhang H. (2016). Up-regulation of REG3A in colorectal cancer cells confers proliferation and correlates with colorectal cancer risk. Oncotarget 7, 3921-3933.

Zhang M.Y., Wang J. and Guo J. (2019). Role of regenerating islet-derived protein 3A in gastrointestinal cancer. Front. Oncol. 9, 1449.

Zhao X., Zhang Y., Deng L., Wang Y., Li Y. and Chen M. (2019). The association between Chinese patients' elevated omentin-1 levels, their clinicopathological features, and the risk of colorectal cancer. Int. J. Clin. Exp. Pathol. 12, 2264-2274.

Zhou J., Tang Z., Gao S., Li C., Feng Y. and Zhou X. (2020). Tumor-associated macrophages: Recent insights and therapies. Front. Oncol. 10, 188.

Zhou S., Jiang H., Wang H., Lu H., Chen R., Xu H., Su Z. and Shao X. (2018). Reg3β from cardiomyocytes regulated macrophage migration, proliferation and functional skewing in experimental autoimmune myocarditis. Ame. J. Clin. Exp. Immunol. 7, 8-15.

Accepted March 29, 2023